SCIENTIFIC REPORTS

OPEN

Binding kinetics of cariprazine and aripiprazole at the dopamine D_3 receptor

Received: 17 May 2018
Accepted: 3 August 2018
Published online: 21 August 2018

Annika Frank[1], Dóra J. Kiss[2,3], György M. Keserű[2] & Holger Stark[1]

The dissociation behaviours of aripiprazole and cariprazine at the human D_2 and D_3 receptor are evaluated. A potential correlation between kinetics and *in vivo* profiles, especially cariprazine's action on negative symptoms in schizophrenia, is investigated. The binding kinetics of four ligands were indirectly evaluated. After the receptor preparations were pre-incubated with the unlabelled ligands, the dissociation was initiated with an excess of [^{3}H]spiperone. Slow dissociation kinetics characterizes aripiprazole and cariprazine at the D_2 receptor. At the D_3 receptor, aripiprazole exhibits a slow monophasic dissociation, while cariprazine displays a rapid biphasic behaviour. Functional ß-arrestin assays and molecular dynamics simulations at the D_3 receptor confirm a biphasic binding behaviour of cariprazine. This may influence its *in vivo* action, as the partial agonist could react rapidly to variations in the dopamine levels of schizophrenic patients and the ligand will not quantitatively dissociate from the receptor in one single step. With these findings novel agents may be developed that display rapid, biphasic dissociation from the D_3R to further investigate this effect on *in vivo* profiles.

Schizophrenia is a group of neurological diseases characterized by specific symptom complexes. Positive symptoms, which are exaggerated in schizophrenic patients, include hallucinations or delusions. Negative symptoms (*e.g.* depression or anhedonia) represent the impairment of healthy cognitive behaviour. The origin of the symptoms is not clarified, but a neurotransmitter dysregulation in different parts of the brain is likely. Hyperactive dopamine transmission and increased D_2 receptor (D_2R) activation may cause positive symptoms. Hypoactive dopamine transmission and hence less D_1 receptor activation in the prefrontal areas may be responsible for negative symptoms[1]. D_3 receptors (D_3Rs) seem to contribute to the origin of negative symptoms[2]. To date schizophrenia is treated only symptomatically. Typical first generation antipsychotic drugs reduce the positive symptoms but display severe and therapy limiting adverse drug effects (ADE) like extrapyramidal motoric symptoms (EPMS). The second generation, also known as atypical antipsychotic drugs reduce these adverse effects, while remain highly effective against positive symptoms. Aripiprazole, an atypical antipsychotic agent, exhibits good efficacy on the positive symptomatic of schizophrenia and a rather beneficial ADE profile. However it is not able to treat the negative symptoms of the disease sufficiently. Cariprazine, a novel antipsychotic agent[3,4], entered the US market in 2016 and obtained European Medicines Agency (EMA) approval in May 2017. Unlike most other antipsychotics it is effective against negative symptoms in clinical trials[5], although the mechanism of this action remains elusive.

Distinct residence times (RTs) are discussed to influence drug profiles *in vivo*[6], although proof of this hypothesis remains pending. As the RT ($1/k_{off}$) determines the duration of receptor occupancy it may influence signalling pathways or ADE[7,8]. Several studies address the RTs of antipsychotic drugs at the D_2R and the correlation to efficacy or ADE[9], however, to date such approaches have not been made for the D_3R. A recent review highlighted the relevance of conformational receptor states and biased signalling at G-protein coupled receptors (GPCRs)[10]. With increasing insights into the crystal structure and signal transduction of GPCRs, it becomes more important to evaluate pharmacological characteristics of novel agents. We hypothesize that cariprazine's dissociation behaviour elucidates possible mechanisms for its action on negative symptoms in schizophrenia. Its profile is compared to the partial agonist aripiprazole, the antagonist spiperone and the agonist rotigotine. In doing so, the

[1]Institute of Pharmaceutical and Medicinal Chemistry, Heinrich Heine University Düsseldorf, Duesseldorf, Germany. [2]Medicinal Chemistry Research Group, Research Centre for Natural Sciences, Hungarian Academy of Sciences, Budapest, Hungary. [3]ELTE Eötvös Loránd University, Doctoral School of Chemistry, Budapest, Hungary. Correspondence and requests for materials should be addressed to G.M.K. (email: keseru.gyorgy@ttk.mta.hu) or H.S. (email: stark@hhu.de)

Drug	k_{off} [min^{-1}] ± s.d. {n}	pK_i ± s.d. (K_i [nM]) {n}
Aripiprazole	0.026 ± 0.001 {3}	8.95 ± 0.06 (1.1) {3}
Cariprazine	0.041 ± 0.002 {3}	8.80 ± 0.12 (1.6) {3}
Rotigotine	0.113 ± 0.029 {3}	7.73 ± 0.10 (18.5) {4}
Spiperone	0.028 ± 0.018 {3}	10.01 ± 0.29 (0.1) {4}

Table 1. D_2R k_{off} and equilibrium dissociation constants (±s.d.) of the unlabelled ligands. pK_i are determined by radioligand displacement assays. $D_{2s}R$ membrane preparations were incubated with [^{3}H]spiperone and the compound. k_{off} are determined by radioligand dilution assays. $D_{2s}R$ membrane preparations were pre-incubated with the compound. Afterwards dissociation was initiated with an excess of [^{3}H]spiperone. Results are means ± s.d. at least performed with n = 3 independent experiments at room temperature.

	Monophasic fit	Biphasic fit		
Drug	k_{off} [min^{-1}] ± s.d. {n}	k_{off1} [min^{-1}] ± s.d. {n}	k_{off2} [min^{-1}] ± s.d. {n}	pK_i ± s.d. (K_i [nM]) {n}
Aripiprazole	0.05 ± 0.02 {3}	0.03 ± 0.02 {3}	0.15 ± 0.08 {3}	8.13 ± 0.19 (7.3) {5}
Cariprazine	0.16 ± 0.04 {9}	0.03 ± 0.01 {8}	0.63 ± 0.38 {8}	9.24 ± 0.18 (0.6) {6}
Rotigotine	0.07 ± 0.02 {4}	0.04 ± 0.02 {3}	0.18 ± 0.01 {3}	8.44 ± 0.26 (3.7) {3}
Spiperone	0.05 ± 0.02 {3}	0.02 ± 0.01 {2}	0.47 ± 0.35 {2}	8.96 ± 0.28 (1.1) {4}

Table 2. D_3R k_{off} and equilibrium dissociation constants (±s.d.) of the unlabelled ligands. pK_i are determined by radioligand displacement assays. D_3R membrane preparations were incubated with [^{3}H]spiperone and the compound. k_{off} are determined by radioligand dilution assays. D_3R membrane preparations were pre-incubated with the compound. Afterwards dissociation was initiated with an excess of [^{3}H]spiperone. Results are means ± s.d. at least performed with n = 3 independent experiments at room temperature. k_{off} displays the k_{off} derived by the monophasic fit, while k_{off1} and k_{off2} are the two k_{off} derived by the biphasic fit.

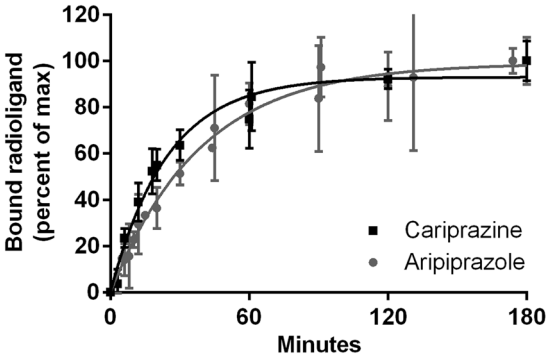

Figure 1. Dissociation of aripiprazole and cariprazine from the D_2R, determined by dilution assays. After pre-incubating $D_{2s}R$ membrane preparations with the compounds, dissociation was initiated with an excess of [^{3}H] spiperone. Figure displays normalized values globally fitted for all experiments (n = 3, triplicates) given as mean with s.d.

understanding of ligand binding to the D_3R could be improved and drug development might benefit from clinically optimized drugs, focused on specific symptoms.

Results

[^{3}H]spiperone kinetic experiments. Dissociation rate constants (k_{off}) of [^{3}H]spiperone are 0.013 min^{-1} (±0.003 min^{-1}) at the D_2R and 0.033 min^{-1} (±0.019 min^{-1}) at the D_3R. The k_{off} of unlabelled spiperone in the indirect assay matches the k_{off} of [^{3}H]spiperone at both receptors (Tables 1 and 2), supporting the applicability of the dilution method.

D_2R kinetic experiments. Aripiprazole and cariprazine share similar RTs at the D_2R with 38 min for aripiprazole and slightly faster (24 min) for cariprazine (Table 1, Fig. 1). These results are in accordance to those of Klein Herenbrink, who found only slight differences at the D_2R[7]. The k_{off} of aripiprazole is concordant with studies performed on rat[8,11] and human receptors[12,13] and the slow dissociation of spiperone[7,14–16] is also corroborated. References, predicting a fast k_{off} of aripiprazole from the D_2R[7,17] and a slow k_{off} for rotigotine[18], are not confirmed. The measured RTs at the D_2R correlate with the drugs' affinities (radioligand displacement assays, pK_i Table 1). Spiperone and aripiprazole (highest affinities) display the longest RTs, while rotigotine (lowest affinity) shows the fastest dissociation from the D_2R. This correlation of binding kinetics and affinities at the D_2R was demonstrated

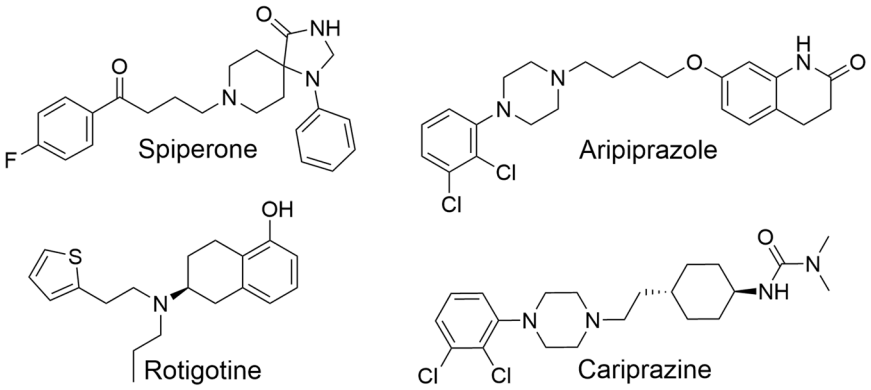

Figure 2. Chemical structures of the evaluated ligands.

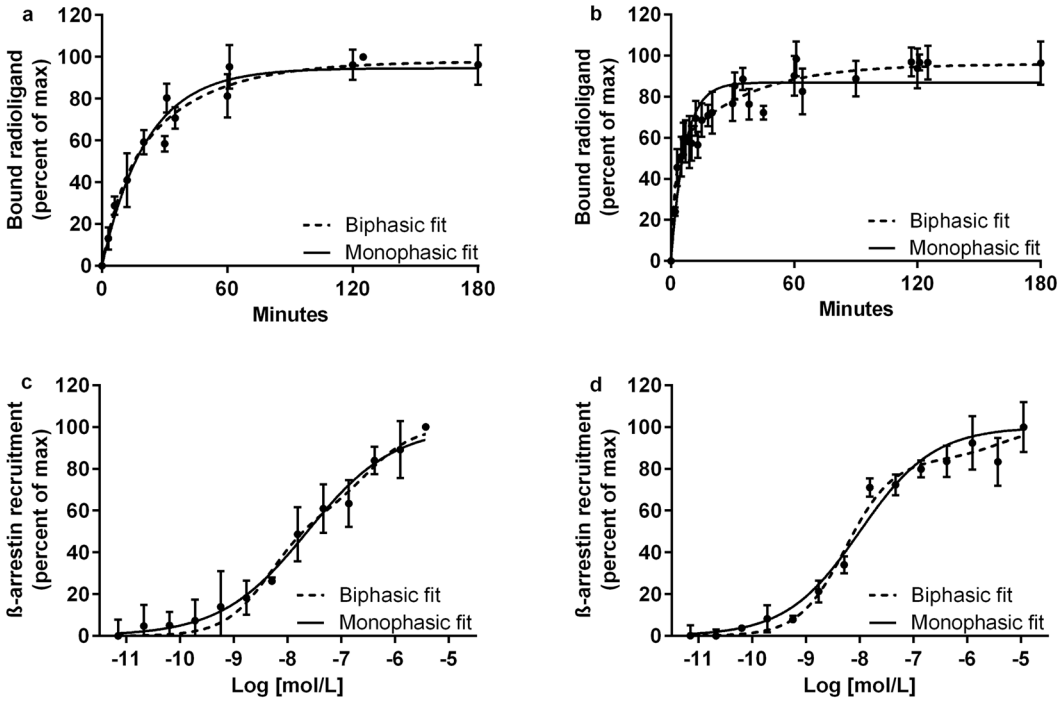

Figure 3. Dissociation profiles and ß-arrestin recruitment of aripiprazole and cariprazine at the D_3R. (**a**,**b**) Dissociation of aripiprazole (**a**) and cariprazine (**b**) from the D_3R, determined by dilution assays. D_3R membrane preparations were pre-incubated with the compounds. Dissociation was initiated with an excess of [^{3}H]spiperone. Figure displays normalized values globally fitted for all experiments (n = 3/9, triplicates) given as mean with s.d. (**c**,**d**) ß-arrestin activation of aripiprazole (**c**) and cariprazine (**d**) at the D_3R. U2OS cells were incubated with partial agonists for 90 min. Data is normalized, globally fitted for all experiments (n = 2, duplicates) given as mean with s.d.

by Kapur and Seeman[14]. Spiperone, aripiprazole and cariprazine (slow k_{off}) share a large, lipophilic aromatic motif, connected through a linker to a second motif with different hydrogen-bond acceptor and donor groups (Fig. 2), while rotigotine is missing this diverse motif. In the presented study the antagonist and the partial agonists display a slow dissociation, while the full agonist rotigotine shows fast dissociation from the D_2R, which is supported by their structural and binding properties.

D_3R kinetic experiments. The evaluation of k_{off} at the D_3R reveals different dissociation behaviours of aripiprazole and cariprazine (Table 2, Fig. 3a,b). Cariprazine displays a rapid biphasic dissociation behaviour ($p < 0.0001$) that is not sufficiently described by a monophasic fit. Dissociation of aripiprazole is slower and better described by a monophasic fit ($p = 0.0925$). Evaluation of the antagonist spiperone also reveals a slow, but biphasic ($p < 0.0001$) dissociation, while the agonist rotigotine displays a monophasic ($p = 0.0688$) dissociation, not significantly faster than aripiprazole or spiperone. The biphasic dissociation of cariprazine is not altered by the

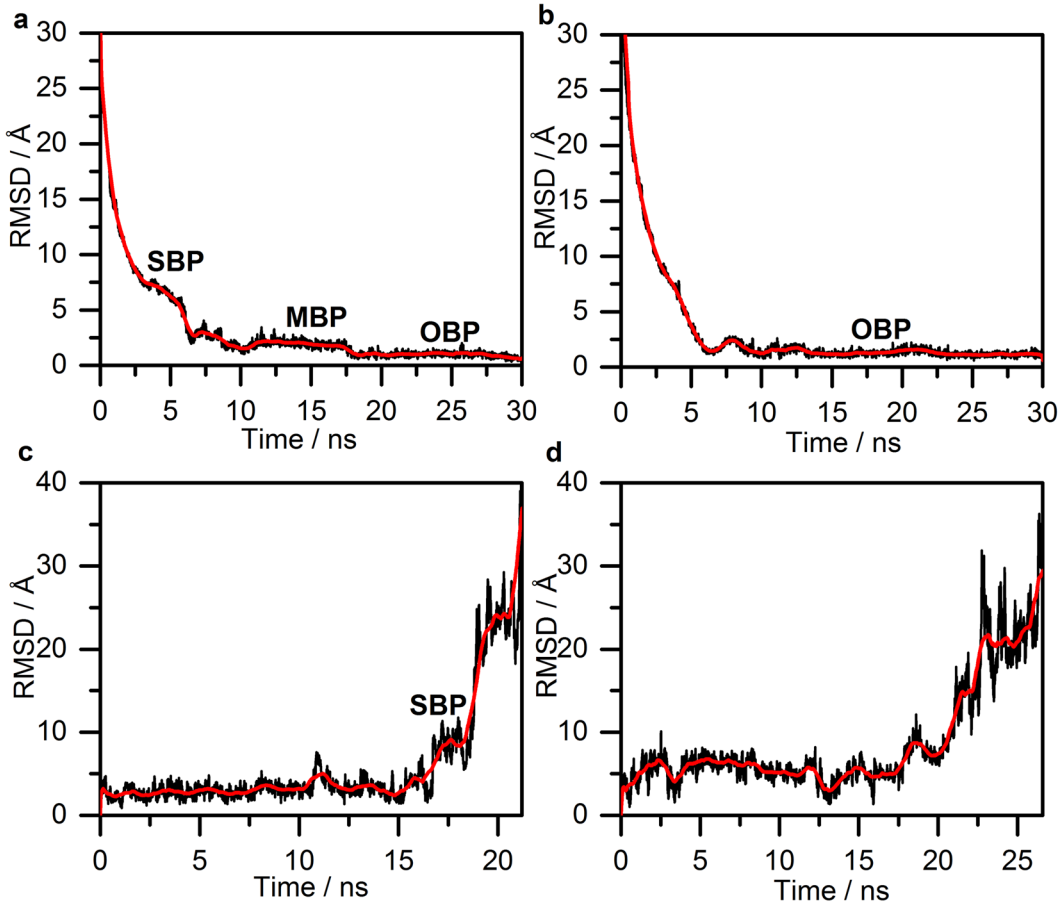

Figure 4. Ligand heavy atom RMSD during the binding (**a**: cariprazine, **b**: aripiprazole) and unbinding (**c**: cariprazine, **d**: aripiprazole) simulations. Black line corresponds to the calculated values, the smoothed curve is calculated as moving average for 100 points for better visualization. The separate phases of the binding are indicated on the graph.

addition of guanosine 5′-[β,γ-imido]triphosphate (Gpp(NH)p), the absence of sodium in the buffer or the use of another radioligand ([^{3}H]raclopride).

Functional binding assays at the D_3R. ß-arrestin 2 recruitment assays result in EC_{50} values of 23.7 nM for aripiprazole and 10.2 nM for cariprazine (monophasic fit). However, a biphasic fit of cariprazine is more appropriate ($p = 0.0004$) with EC_{50} values of 5.52 nM and 4.19 µM (Fig. 3c,d). Both are partial agonist in the tested system with ca. 30% of E_{max}. A statistically non-significant biphasic binding is observed for cariprazine in radioligand displacement studies with pK_i of 8.71 and 11.91. In case of aripiprazole, the biphasic fit is not applicable.

Molecular Modelling. The root-mean-square deviation of atomic positions (RMSD) against the time-frame in binding trajectories are consistent with the observed biphasic kinetics of cariprazine (Fig. 4a) and the one-phase kinetics of aripiprazole (Fig. 4b). Upon reaching the receptor surface cariprazine contacts extracellular loop (ECL) 2 and ECL1, which are guiding it towards the entrance of the binding site. The 3–5 ns period (Fig. 4a) corresponds to the secondary binding pose (SBP), where cariprazine interacts with extracellular surface residues, mainly on ECL2, the top part of the transmembrane region (TM) 2 and TM5-7 (Fig. 5a). Key hydrogen-bonds (H-bonds) with Ser182^{ECL2} and Glu2.65 and hydrophobic interactions (*e.g.* Val5.39, Pro5.36) contribute to the stabilization (Fig. 5e). Tyr7.35 helps to isolate the ligand from the orthosteric binding site. After 5 ns cariprazine rearranges in the receptor cavity, enters the orthosteric site, transiently stabilized in a metastable binding pose (MBP, 10–17.5 ns, Fig. 4a) then reaches the final, orthosteric binding pose (OBP, 20–30 ns, Fig. 4a). These two positions resemble regarding the orientation of the ligand (Fig. 5b,c), however the occupancy of the key H-bond interaction with Asp3.32 increases from 10% (MBP) to 99% (OBP). Hydrophobic interactions (e.g. Val3.33, Ile183^{ECL2}, Phe6.51, Phe5.38, Leu2.64 and Tyr7.35) also contribute to the stabilization (Fig. 5e) of the binding mode. Similar to previous molecular dynamic (MD) studies of D_3R ligands[19], Tyr7.35 and the ECL2 residues Ser182, Ile183, Ser184 function as a lock, facilitating the entrance of the ligand into the binding pocket (Fig. 6). The recently published high resolution structure of the D_2R confirms the impact of Ile184 (Ile183 in the D_3R) on the binding kinetics of bivalent ligands (ligands bearing two pharmacophores connected by a linker[13,20–22]). Aripiprazole also first interacts with the ECL2 of the receptor, then forms a π–π stacking interaction with Tyr7.35. The lock opens and the ligand enters the binding site. A stable intermediate state was not observed (Fig. 4b); the

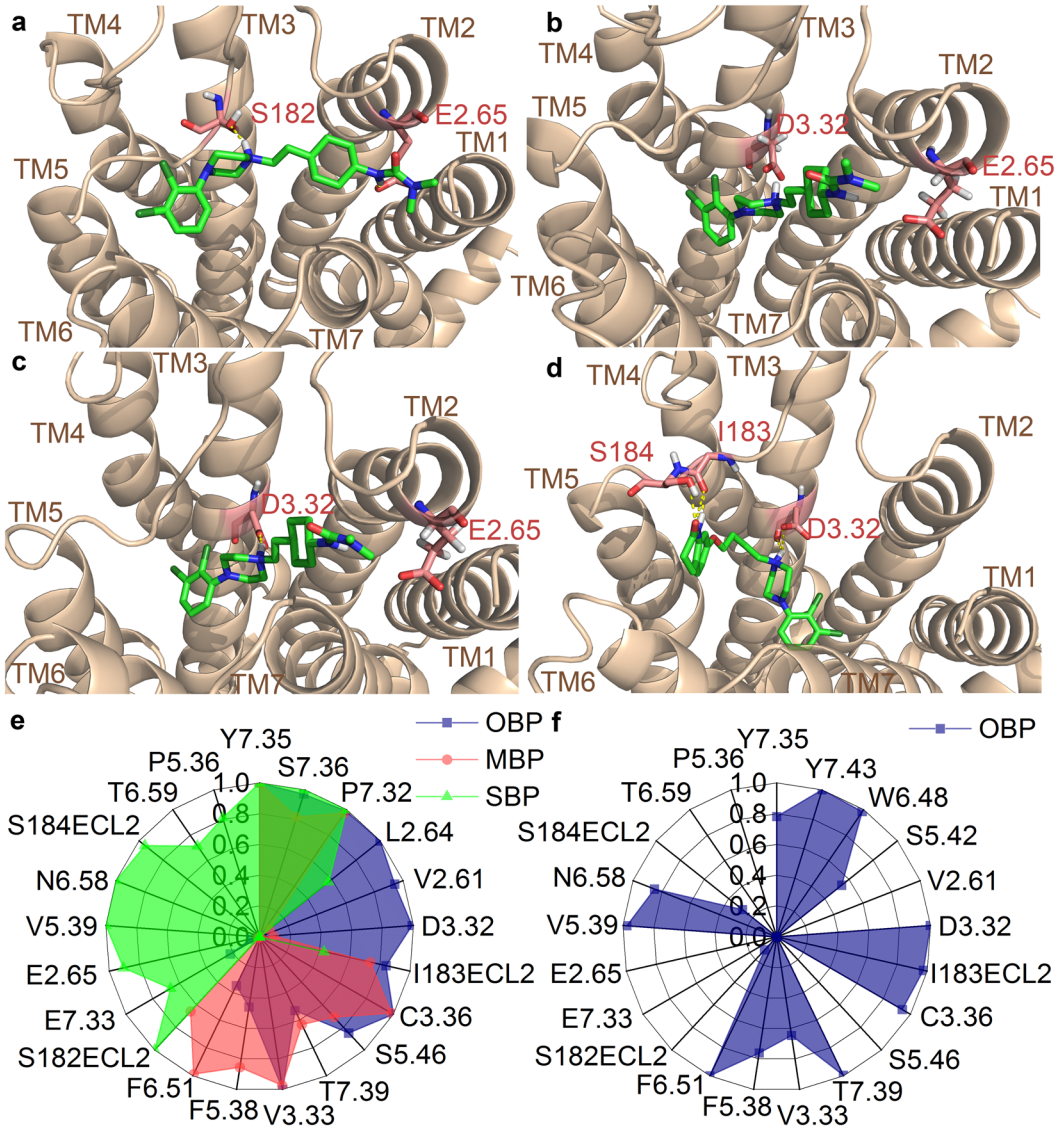

Figure 5. Binding poses and frequent interactions during binding simulations. (**a**–**d**) Cariprazine in the secondary binding pose (**a**, SBP), metastable binding pose (**b**, MBP) and the final binding pose (**c**, OBP) and aripiprazole's final binding pose (**d**, OBP). The complexes are visualized from the top, the protein is represented as ribbon, the ligands as green sticks and important residues as light red sticks. Hydrogen bonds are shown as dashed yellow lines. (**e**,**f**) Most frequent interactions of cariprazine in the SBP (**e**, green), MBP (**e**, red) and OBP (**e**, blue) and aripiprazole in the OBP (**f**, blue).

ligand proceeds till it reaches the OBP and forms the H-bond interaction with Asp3.32, which remains intact (10–30 ns). The orientation of the ligand (Fig. 5d) varies compared to cariprazine, but similar interactions were also detected (Fig. 5f). Both H-bonds (Asp3.32, Ile183^{ECL2}) and hydrophobic interactions (e.g. Trp6.48, Phe6.51, Tyr7.43) stabilize its binding mode. Stability assessments and unbinding simulations suggest that aripiprazole might also reorient in the binding pocket to a similar pose as cariprazine.

Even though the unbinding simulations offer less reliable structural insight, the trajectories display some characteristic dissociation features. Cariprazine relocates into the SBP after 17 ns (Fig. 4c) and fully dissociates after 21 ns. During the unbinding of aripiprazole (Fig. 4d) we could not observe well defined stages, the higher fluctuations in the RMSD values show less stabilization and the shape of the graph resembles more a one-phase dissociation kinetics.

Discussion

Cariprazine and aripiprazole display similar dissociation behaviours at the D_2R, but differ at the D_3R. Aripiprazole exhibits similar RT at the D_3R and the D_2R, whereas cariprazine shows the shortest RT and the most pronounced biphasic behaviour of the tested ligands at the D_3R. This could influence cariprazine's *in vivo* action, as it can react rapidly to variations in the dopamine level. Recent research revealed that metastable receptor states may determine binding orientation of bivalent drugs in MD simulations[22] and may influence their

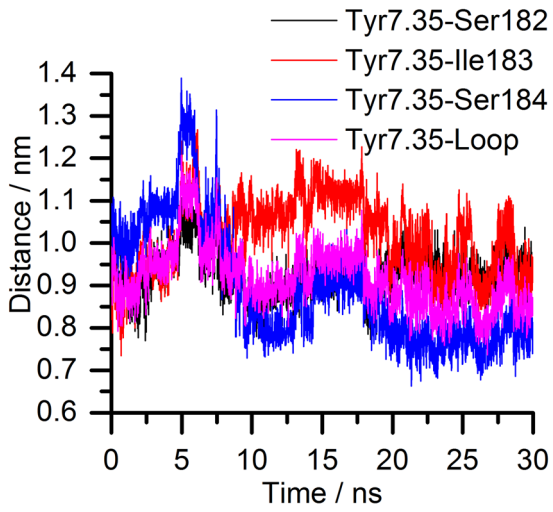

Figure 6. Tyr7.35 and ECL2 lock movement during the binding of cariprazine. Distances between the centre of masses of Tyr7.35 and ECL2 residues Ser182, Ile183, Ser184 and the centre of mass of the three residues together representing the loop position in the cariprazine binding trajectory to the D_3R.

binding kinetics[23]. Our findings suggest that cariprazine's biphasic properties are connected to a metastable binding pose. Different binding poses may influence a biased agonism at the D_3R, by stimulating different signalling pathways depending on the natural ligand's concentration. It has to be mentioned that there may be other explanations for the biphasic *in vitro* behaviour. Given the high affinity and the fast k_{off} from the D_3 receptor, the k_{obs} should be fast, which could result in rebinding effects in the assay. To check this possibility, different concentrations of cariprazine (0.2 and 40 times K_i value, $n = 1$) were evaluated, however, the biphasic nature of its dissociation remained. Although other models may also describe the obtained data, the combination of the experimental data and the MD simulations strengthen a biphasic *in vitro* dissociation profile of cariprazine and a pronounced interaction with different receptor sites. Various studies have shown that the ß-arrestin pathway at the D_2R plays an important role in clinical efficacy of antipsychotics. Genetic ß-arrestin depletion led to a loss in antipsychotic activity of tested agents with an increase in motoric ADE[24]. A BRET assay revealed the antagonism of antipsychotic drugs, including aripiprazole, on the D_2R mediated ß-arrestin recruitment[25]. Given the biphasic nature of cariprazines ß-arrestin recruitment and dissociation from the D_3R, increases in local dopamine concentration may not lead to a complete displacement of the ligand, but a certain amount will be able to act at the target for a longer period.

A recent review[26] criticizes the use of the RT as sole explanation of a drug's profile and claims for individual evaluation of its impact. In the case of antipsychotic agents however, the correlation between RT and drug profiles seems to be a reasonable hypothesis for different *in vivo* profiles[9]. Cariprazine displays a different dissociation profile than other tested ligands and shows concurring properties in functional assays and MD simulations at the D_3R. Its profile differs especially from aripiprazole, also a highly active antipsychotic, only lacking the effectivity on the negative symptoms. Therefore, the characteristic receptor interaction may be one possible cause behind the efficacy of cariprazine on the negative symptoms of schizophrenia.

Although the clinical effects of cariprazine seem to correlate to its binding behaviour at the D_3R, there may be additional factors. The translation of an *in vitro/in silico* biphasic behaviour to *in vivo* effects remains to be elucidated and requires more research on the origin of negative symptoms. However, with these findings, it is possible to rationally develop compounds with biphasic kinetics and characterize them *in vivo* regarding their effects on the negative symptomatic. Within this work, we show that:

- Cariprazine and aripiprazole share similar dissociation properties at the D_2R
- Cariprazine and aripiprazole display different dissociation profiles at the D_3R
- Cariprazine dissociates faster from the D_3R than from the D_2R
- Cariprazine exhibits biphasic kinetics at the D_3R
- The biphasic behaviour is also observed in functional assays with cariprazine
- MD simulations support the experiments with structural interpretation.

Recent work[13] emphasizes the significance of evaluating and comparing binding modes to understand and advance drug development. By elucidating the binding profile of cariprazine the insights on receptor interaction at the D_3R were broadened and future evaluation of novel antipsychotic drugs with special focus on the negative symptoms has gained an interesting aspect. By this, a next step in the understanding and improvement of antipsychotic therapy was made and future approaches may benefit from specialized agents for this diverse symptom complex.

Methods

Cell culture and membrane preparation of CHO cells expressing the $hD_{2s}R$ and the hD_3R. Cell culture and membrane preparations were performed as reported previously with modifications[27]. CHO cells stably expressing the human dopamine $D_{2short}R$ or D_3R were cultured in DMEM (with 1% glutamine, 10% FBS, and 1% penicillin/streptomycin for D_2; 1% glutamine, 10% dialysed FBS for D_3). CHO-D_2 cells were collected in PBS buffer, CHO-D_3 cells in medium and centrifuged at 3,000 × g for 10 min at 4 °C. The pellet was resuspended in binding buffer (1 mM $MgCl_2$, 1 mM $CaCl_2$, 5 mM KCl, 120 mM NaCl and 50 mM Tris, pH 7.7), disrupted and centrifuged at 23,000 × g for 30 min (4 °C). The resulting pellet was stored in binding buffer at −80 °C.

Radioligand displacement assays at the hD_2R and the hD_3R. Displacement assays were performed as reported previously[28] with modifications. Briefly, membrane preparations ($D_{2s}R$: 25 µg/well; D_3R: 20 µg/well) were co-incubated with [^{3}H]spiperone (0.2 nM) and the test ligand. Nonspecific binding (NSB) was measured with haloperidol (10 µM) and separation of bound radioligand was performed using VE-water. Assays ran in triplicates at least in three independent experiments. Data was analysed using non-linear regression and equation "one site competition". The K_i values were calculated from the IC_{50} values using the Cheng-Prusoff equation[29].

Determination of the [^{3}H]spiperone dissociation rate constants at the D_2R and the D_3R. The k_{off} of [^{3}H]spiperone (RL) was measured, using an excess of haloperidol[30]. Cell preparations ($D_{2s}R$: 25 µg/well; D_3R: 20 µg/well) were incubated (120 min, 250 rpm) with 0.2 nM RL in 0.2 mL. The dissociation was initiated at different time points with an excess of haloperidol (0.4 mM stock, 15 µL to prevent dilution). Assays ran in quadruplicates with eleven time points with $n = 4$ at the D_2R and $n = 7$ at the D_3R. NSB was determined with haloperidol (10 µM), total binding with 0.2 nM RL for the total time of the experiments. Bound RL was separated as described above. Binding data was analysed using non-linear regression and fitting to "one phase exponential decay".

Determination of unlabelled ligands dissociation rate constants at the D_2R and the D_3R. The k_{off} of unlabelled ligands (UL) were measured indirectly by the dilution method, similar as described previously[30,31]. 50 µL of the membrane preparations ($D_{2s}R$: 25 µg/well; D_3R: 20 µg/well) were incubated with the UL at four times its K_i value for 120 min. Afterwards the dissociation was initiated at different time points with an excess of RL (150 µL, 20 times its K_D value). This dilution results in the majority of the receptors being occupied by RL at the end of the experiment. As the RL may only bind when the UL has dissociated, k_{obs} of the RL reflects the k_{off} of the UL (Supplementary Fig. S1). To ensure, that the association of the RL occurs without delay to the dissociation of the UL, the concentration of the RL has to be very high (*e.g.* 20 times K_D value). This model assumes that RL and UL bind to the same binding site. Assays ran in triplicates with eight time points with at least $n = 3$ independent experiments. Total binding was measured in the absence of UL; at the end of the experiments 80–100% of the total binding were achieved (spiperone and rotigotine 70% at the D_3R). Rotigotine was measured at 5 times its K_i value at the D_3R. NSB and separation are described above. The k_{off} were obtained by applying non-linear regression and fitting to "one phase exponential association" or "two phase exponential association". As this indirect method underlies model theories and assumptions the resulting k_{off} are approximations that serve mainly as comparison criteria. The effects of Gpp(NH)p, the omitting of sodium-ions in the buffer and of using [^{3}H]raclopride as RL were evaluated with the same method ($n \geq 2$).

Measurement of ß-arrestin 2 activation at the D_3R by aripiprazole and cariprazine. The PathHunter® ß-arrestin eXpress GPCR assay kit was used to measure ß-arrestin recruitment at the D_3R (protocol of agonists for aripiprazole and cariprazine). Briefly, U2OS cells were incubated at 37 °C for 48 h. Agonist dilutions were added to the respective wells and incubated for 90 min at 37 °C. Afterwards the detection reagent was added and incubated for 60 min at room temperature in the dark. Luminescence was read with the Infinite 1000 Reader (Tecan). Assays ran in duplicates with $n = 2$ independent experiments. Data was analysed using non-linear regression and fitting to equations "log(agonist) vs. normalized response - variable slope" and "biphasic". For biphasic fitting "bottom" was constrained to zero, "top" to 100 and nH1/nH2 to 1.

Molecular modelling approaches at the D_3R. MD simulations were performed on cariprazine and aripiprazole. The initial structures were constructed from the D_3R X-Ray structure (Protein database entry code: 3PBL)[32], mutated residues were transformed to their natural form, eticlopride was removed. The protein was embedded into a 1-palmitoyl-2-oleoyl-sn-glycero-3-phosphocholine (POPC) lipid bilayer, the complexes were solvated in TIP3P waters and neutralized with chloride ions. Parameterization was based on Amber ff14SB force field[33] and restrained electrostatic potential (RESP)[34] charges were calculated for the ligands. All preparatory steps were carried out with the default parameters in the BiKi Life Sciences suite[35]. The structures were minimized and equilibrated following the default protocol of the program package (see details in the Supplementary Information). Binding studies against the D_3R were carried out applying BiKi Life Sciences MD Binding tool implemented in GROMACS-4.6.1[36] as published recently[37]. This approach is based on adaptive forces attracting the ligand into the predefined binding site, which residues were identified by NanoShaper[38] and refined by visual inspection (Supplementary Table S1). The additional attractive forces between the ligand and the binding site facilitate the ligand to overcome the barrier of entering the binding pocket; therefore reduce the timescale of the full binding event into a few 10 ns. The bias was switched off, when the ligand reached the 4 Å distance criteria from the backbone heavy atoms of Ser193. During the 20 replica production runs an 0.2 gaining factor was applied in the 30 ns long simulations in isothermal-isobaric (NPT) ensemble at 300 K and 1.013 bar pressure. The binding poses lacking hydrogen bond interaction with the conserved Asp110 were ruled out, the remaining unbiased trajectories were clustered with GROMACS g_cluster tool by the single-linkage method (1.5 Å cut-off) and their stability was tested with scaled MD. The most stable pose was identified as final binding mode and the

interaction fingerprints were calculated by IChem[39] with default settings based on every 10th frame of the corresponding trajectories. The unbinding studies were based on scaled MDs with a scaling factor of 0.4 applying BiKiNetics tool[40]. The final binding mode of the MD binding simulations was the starting pose using structural restraints in canonical (NVT) ensemble at 300 K without the explicit membrane environment. The applied parameters are summarized in Supplementary Table S1. The ligands were considered fully dissociated, when the 6 Å solvation shell around them contained only water molecules.

Data and statistical analysis. *In vitro* assays were analysed with Prism 6 (GraphPad Software Inc., San Diego, CA) and are given as means ± standard deviation (s.d.). In some instances the number of experiments was increased to characterize binding properties into detail (*e.g.* biphasic dissociation of cariprazine). This is marked in the tables. The signal of the indirect kinetic experiments and the ß-arrestin assays were normalized (zero was set as zero) to allow comparison of different curve shapes. Significance of biphasic fitting over one-phasic fitting or "biphasic" over "log(agonist) vs. normalized response" was tested with the globalized data sets using the "extra sum-of-squares F Test" provided by GraphPad. Comparisons were considered significant if p-value was <0.05 ($\alpha = 0.05$). All *in vitro* assays were performed at room temperature.

Materials and reagents. [^{3}H]Radioligands were purchased from Perkin Elmer (Waltham, USA). Cariprazine was synthesized at RCNS, Hungary. The authors confirm the identity and purity of the given compound. The ß-arrestin kit was purchased from DiscoverX (Birmingham, UK).

Data availability. The datasets generated and analysed during the current study are available from the corresponding author on reasonable request.

References

1. Brisch, R. *et al*. The role of dopamine in schizophrenia from a neurobiological and evolutionary perspective: old fashioned, but still in vogue. *Front. Psychiatry* **5**, 47, https://doi.org/10.3389/fpsyt.2014.00047 (2014).
2. Sokoloff, P. & Le Foll, B. The dopamine D3 receptor, a quarter century later. *Eur. J. Neurosci.* **45**, 2–19 (2017).
3. Ágai-Csongor, É. *et al*. Discovery of cariprazine (RGH-188): a novel antipsychotic acting on dopamine D3/D2 receptors. *Bioorg. Med. Chem. Lett.* **22**, 3437–3440 (2012).
4. Wesołowska, A., Partyka, A., Jastrzębska-Więsek, M. & Kołaczkowski, M. The preclinical discovery and development of cariprazine for the treatment of schizophrenia. *Expert Opin. Drug Discov*. in press, 1471057; https://doi.org/10.1080/17460441.2018.1471057 (2018).
5. Németh, G. *et al*. Cariprazine versus risperidone monotherapy for treatment of predominant negative symptoms in patients with schizophrenia: a randomised, double-blind, controlled trial. *Lancet* **389**, 1103–1113 (2017).
6. Copeland, R. A. Thermodynamics and Binding Kinetics in Drug Discovery [Keserü, G. M. & Swinney, D. C. (ed.)] *Thermodynamics and Kinetics of Drug Binding*, 157–167 (Wiley Online Library, 2015).
7. Klein Herenbrink, C. *et al*. The role of kinetic context in apparent biased agonism at GPCRs. *Nat. Commun.* **7**, 10842, https://doi.org/10.1038/ncomms10842 (2016).
8. Carboni, L. *et al*. Slow dissociation of partial agonists from the D(2) receptor is linked to reduced prolactin release. *Int. J. Neuropsychopharmacol.* **15**, 645–656 (2012).
9. Vauquelin, G., Bostoen, S., Vanderheyden, P. & Seeman, P. Clozapine, atypical antipsychotics, and the benefits of fast-off D2 dopamine receptor antagonism. *Naunyn Schmiedebergs Arch. Pharmacol.* **385**, 337–372 (2012).
10. Hauser, A. S., Attwood, M. M., Rask-Andersen, M., Schiöth, H. B. & Gloriam, D. E. Trends in GPCR drug discovery: New agents, targets and indications. *Nat. Rev. Drug Discov.* **16**, 829–842 (2017).
11. Roth, B. L., Sheffler, D. & Potkin, S. G. Atypical antipsychotic drug actions: unitary or multiple mechanisms for 'atypicality'? *Clin. Neurosci. Res.* **3**, 108–117 (2003).
12. Langlois, X. *et al*. Pharmacology of JNJ-37822681, a specific and fast-dissociating D2 antagonist for the treatment of schizophrenia. *J. Pharmacol. Exp. Ther.* **342**, 91–105 (2012).
13. Wang, S. *et al*. Structure of the D2 dopamine receptor bound to the atypical antipsychotic drug risperidone. *Nature* **555**, 269–273 (2018).
14. Kapur, S. & Seeman, P. Antipsychotic agents differ in how fast they come off the dopamine D2 receptors. Implications for atypical antipsychotic action. *J. Psychiatry. Neurosci.* **25**, 161–166 (2000).
15. Leysen, J. E. & Gommeren, W. The dissociation rate of unlabelled dopamine antagonists and agonists from the dopamine-D2 receptor, application of an original filter method. *J. Recept. Res.* **4**, 817–845 (1984).
16. Sibley, D. R., Mahan, L. C. & Creese, I. Dopamine receptor binding on intact cells. Absence of a high-affinity agonist-receptor binding state. *Mol. Pharmacol.* **23**, 295–302 (1983).
17. Seeman, P. Targeting the dopamine D2 receptor in schizophrenia. *Expert. Opin. Ther. Targets* **10**, 515–531 (2006).
18. Wood, M., Dubois, V., Scheller, D. & Gillard, M. Rotigotine is a potent agonist at dopamine D1 receptors as well as at dopamine D2 and D3 receptors. *Br. J. Pharmacol.* **172**, 1124–1135 (2015).
19. Thomas, T., Fang, Y., Yuriev, E. & Chalmers, D. K. Ligand binding pathways of clozapine and haloperidol in the dopamine D2 and D3 receptors. *J. Chem. Inf. Model.* **56**, 308–321 (2016).
20. Bonifazi, A. *et al*. Novel bivalent ligands based on the sumanirole pharmacophore reveal Dopamine D2 Receptor (D2R) biased agonism. *J. Med. Chem.* **60**, 2890–2907 (2017).
21. Lane, J. R., Sexton, P. M. & Christopoulos, A. Bridging the gap: Bitopic ligands of G-protein-coupled receptors. *Trends Pharmacol. Sci.* **34**, 59–66 (2013).
22. Strasser, A., Wittmann, H.-J. & Seifert, R. Binding kinetics and pathways of ligands to GPCRs. *Trends Pharmacol. Sci.* **38**, 717–732 (2017).
23. Lane, J. R. *et al*. Structure-based ligand discovery targeting orthosteric and allosteric pockets of dopamine receptors. *Mol. Pharmacol.* **84**, 794–807 (2013).
24. Allen, J. A. *et al*. Discovery of β-arrestin–biased dopamine D2 ligands for probing signal transduction pathways essential for antipsychotic efficacy. *Proc. Natl. Acad. Sci. USA* **108**, 18488–18493 (2011).
25. Masri, B. *et al*. Antagonism of dopamine D2 receptor/β-arrestin 2 interaction is a common property of clinically effective antipsychotics. *Proc. Natl. Acad. Sci. USA* **105**, 13656–13661 (2008).
26. Folmer, R. H. A. Drug target residence time: a misleading concept. *Drug Discov. Today* **23**, 12–16 (2018).
27. Sokoloff, P. *et al*. Pharmacology of human dopamine D3 receptor expressed in a mammalian cell line: comparison with D2 receptor. *Eur. J. Pharmacol.* **225**, 331–337 (1992).

28. Schübler, M., Sadek, B., Kottke, T., Weizel, L. & Stark, H. Synthesis, molecular properties estimations, and dual dopamine D2 and D3 receptor activities of benzothiazole-based ligands. *Front. Chem.* **5**, 64, https://doi.org/10.3389/fchem.2017.00064 (2017).
29. Yung-Chi, C. & Prusoff, W. H. Relationship between the inhibition constant (Ki) and the concentration of inhibitor which causes 50 per cent inhibition (IC50) of an enzymatic reaction. *Biochem. Pharmacol.* **22**, 3099–3108 (1973).
30. Bosma, R., Mocking, T. A.M., Leurs, R. & Vischer, H. F. Ligand-Binding Kinetics on Histamine Receptors [Tiligada, E. & Ennis, M. (ed.)] *Histamine Receptos as Drug Targets*, 115–155 (Springer Science + Business Media LLC, New York, USA).
31. Swinney, D. C. *et al*. A study of the molecular mechanism of binding kinetics and long residence times of human CCR5 receptor small molecule allosteric ligands. *Br. J. Pharmacol.* **171**, 3364–3375 (2014).
32. Chien, E. Y. T. *et al*. Structure of the human dopamine D3 receptor in complex with a D2/D3 selective antagonist. *Science* **330**, 1091–1095 (2010).
33. Maier, J. A. *et al*. ff14SB: Improving the accuracy of protein side chain and backbone parameters from ff99SB. *J. Chem. Theor. Comp.* **11**, 3696–3713 (2015).
34. Bayly, C. I., Cieplak, P., Cornell, W. & Kollman, P. A. A well-behaved electrostatic potential based method using charge restraints for deriving atomic charges: the RESP model. *J. Phys. Chem.* **97**, 10269–10280 (1993).
35. Decherchi, S., Bottegoni, G., Spitaleri, A., Rocchia, W. & Cavalli, A. BiKi Life Sciences: a new suite for molecular dynamics and related methods in drug discovery. *J. Chem. Inf. Model.* **58**, 219–224 (2018).
36. Pronk, S. *et al*. GROMACS 4.5: A high-throughput and highly parallel open source molecular simulation toolkit. *Bioinformatics* **29**, 845–854 (2013).
37. Spitaleri, A., Decherchi, S., Cavalli, A. & Rocchia, W. Fast dynamic docking guided by adaptive electrostatic bias: the MD-Binding approach. *J. Chem. Theor. Comp.* **14**, 1727–1736 (2018).
38. Decherchi, S. & Rocchia, W. A general and robust ray-casting-based algorithm for triangulating surfaces at the nanoscale. *PloS one* **8**, e59744 (2013).
39. Marcou, G. & Rognan, D. Optimizing fragment and scaffold docking by use of molecular interaction fingerprints. *J. Chem. Inf. Model.* **47**, 195–207 (2007).
40. Mollica, L. *et al*. Kinetics of protein-ligand unbinding via smoothed potential molecular dynamics simulations. *Sci. Rep.* **5**, 11539, https://doi.org/10.1038/srep11539 (2015).

Acknowledgements

The authors thank Andrea Cavalli and Sergio Decherchi (Instituto Italiano di Tecnologia (IIT)) for providing access to Biki Life Sciences software and their suggestions, Didier Rognan for providing the license of IChem and the National Information Infrastructure Development (NIIF) Programme for providing us access to the supercomputers in Hungary. CHO-D_{2s} cells were a kind donation of Prof. Dr. Shine (Garvan Institute, Australia). CHO-D_3 cells were donated by Prof. Dr. Sokoloff (Centre Paul Broca de l´INSERM, France). AF and HS participate in the DFG GRK2158- "Natural products and natural product analogs against therapy-resistant tumors and microorganism". D.J.K., G.M.K. and H.S. participated in COST Action CM1207 – "GLISTEN: GPCR-ligand interactions, structures, and transmembrane signalling". D.J.K. and G.M.K. were supported by the National Brain Research Program (2017-1.2.1-NKP-2017-00002). H.S. was kindly supported by DFG INST208/664 and COST Action CA15135. The authors thank S. Hagenow, D. Reiner and M. Frank for scientific discussion.

Author Contributions

A.F. designed, performed and interpreted the radioligand and ß-arrestin assays and wrote the paper; D.J.K. performed and analysed the simulations and contributed to the paper; G.M.K. contributed to the design and interpretation of studies and the paper; H.S. contributed to the design and interpretation of studies and the paper. He also supervised the project. All authors reviewed the manuscript.

Additional Information

Supplementary information accompanies this paper at https://doi.org/10.1038/s41598-018-30794-y.

Competing Interests: G.M.K. contributed to the discovery of cariprazine. The other authors declare no competing interests.

Publisher's note: Springer Nature remains neutral with regard to jurisdictional claims in published maps and institutional affiliations.